

Weakly deformed oblate structures in  $^{198}_{76}\text{Os}_{122}$ 

Zs. Podolyák,<sup>1,\*</sup> S. J. Steer,<sup>1</sup> S. Pietri,<sup>1</sup> F. R. Xu,<sup>2</sup> H. L. Liu,<sup>2</sup> P. H. Regan,<sup>1</sup> D. Rudolph,<sup>3</sup> A. B. Garnsworthy,<sup>1,4</sup> R. Hoischen,<sup>3,5</sup> M. Górska,<sup>5</sup> J. Gerl,<sup>5</sup> H. J. Wollersheim,<sup>5</sup> T. Kurtukian-Nieto,<sup>6</sup> G. Benzoni,<sup>7</sup> T. Shizuma,<sup>1,8</sup> F. Becker,<sup>5</sup> P. Bednarczyk,<sup>5,9</sup> L. Caceres,<sup>5,10</sup> P. Doornenbal,<sup>5</sup> H. Geissel,<sup>5</sup> J. Grębosz,<sup>5,9</sup> A. Kelic,<sup>5</sup> I. Kojouharov,<sup>5</sup> N. Kurz,<sup>5</sup> F. Montes,<sup>5</sup> W. Prokopowicz,<sup>5,9</sup> T. Saito,<sup>5</sup> H. Schaffner,<sup>5</sup> S. Tashenov,<sup>5</sup> A. Heinz,<sup>4</sup> M. Pfützner,<sup>11</sup> A. Jungclaus,<sup>10</sup> D. L. Balabanski,<sup>12</sup> C. Brandau,<sup>1</sup> A. M. Bruce,<sup>13</sup> W. N. Catford,<sup>1</sup> I. J. Cullen,<sup>1</sup> Zs. Dombrádi,<sup>14</sup> E. Estevez,<sup>6</sup> W. Gelletly,<sup>1</sup> G. Ilie,<sup>15</sup> J. Jolie,<sup>15</sup> G. A. Jones,<sup>1</sup> M. Kmiecik,<sup>9</sup> F. G. Kondev,<sup>16</sup> R. Krücken,<sup>17</sup> S. Lalkowski,<sup>13</sup> Z. Liu,<sup>1</sup> A. Maj,<sup>9</sup> S. Myalski,<sup>9</sup> S. Schwertel,<sup>17</sup> P. M. Walker,<sup>1</sup> E. Werner-Malento,<sup>5,18</sup> and O. Wieland<sup>7</sup>

<sup>1</sup>*Department of Physics, University of Surrey, Guildford GU2 7XH, United Kingdom*

<sup>2</sup>*Department of Technical Physics, Peking University, Beijing 100871, People's Republic of China*

<sup>3</sup>*Department of Physics, Lund University, S-22100 Lund, Sweden*

<sup>4</sup>*WNSL, Yale University, New Haven, Connecticut 06520-8124, USA*

<sup>5</sup>*GSI, Planckstrasse 1, D-64291 Darmstadt, Germany*

<sup>6</sup>*Universidad de Santiago de Compostela, E-15706 Santiago de Compostela, Spain*

<sup>7</sup>*INFN, Università degli Studi di Milano, I-20133 Milano, Italy*

<sup>8</sup>*Japan Atomic Energy Agency, Kyoto 619-0215, Japan*

<sup>9</sup>*The Henryk Niewodniczański Institute of Nuclear Physics, PL-31-342 Kraków, Poland*

<sup>10</sup>*Departamento de Física Teórica, Universidad Autónoma de Madrid, E-28049 Madrid, Spain*

<sup>11</sup>*IEP, Warsaw University, Hoża 69, PL-00-681 Warsaw, Poland*

<sup>12</sup>*Institute for Nuclear Research and Nuclear Energy, Bulgarian Academy of Sciences, BG-1784 Sofia, Bulgaria*

<sup>13</sup>*School of Engineering, University of Brighton, Brighton BN2 4GJ, United Kingdom*

<sup>14</sup>*Institute for Nuclear Research, ATOMKI, H-4001 Debrecen, Hungary*

<sup>15</sup>*IKP, Universität zu Köln, D-50937 Köln, Germany*

<sup>16</sup>*Nuclear Engineering Division, Argonne National Laboratory, Argonne, Illinois 60439, USA*

<sup>17</sup>*Physik Department E12, Technische Universität München, Garching, Germany*

<sup>18</sup>*Institute of Physics PAS, Al. Lotnikow 32/46, PL-02-668 Warsaw, Poland*

(Received 23 January 2009; published 16 March 2009)

Gamma rays de-exciting isomeric states in the neutron-rich nucleus  $^{198}_{76}\text{Os}_{122}$  have been observed following relativistic projectile fragmentation of a 1 GeV per nucleon  $^{208}\text{Pb}$  beam. The ground-state band has properties compatible with oblate deformation. The evolution of the structure of Os isotopes characterized by sudden prolate-oblate shape change is discussed and contrasted with the smooth change known in the Pt chain.

DOI: [10.1103/PhysRevC.79.031305](https://doi.org/10.1103/PhysRevC.79.031305)

PACS number(s): 25.70.Mn, 21.10.Re, 27.80.+w

The neutron-rich W-Os-Pt region is characterized by the presence of nuclei with different shapes in their ground states, such as prolate, oblate, triaxial, and spherical. Shape transitional nuclei are difficult to treat theoretically; consequently, this region is considered to be a crucial testing ground for nuclear models. The lighter isotopes are prolate deformed, and by adding more and more neutrons the shape becomes oblate [1,2]. As the  $N = 126$  closed shell is approached the nuclei become spherical [3,4]. In the prolate-oblate transition region the nuclei can be described by a potential with similar energy minima corresponding to prolate and oblate shapes. For the tungsten ( $Z = 74$ ) nuclei a sudden prolate-to-oblate shape change is predicted to happen at around mass 190–192 [1,2], with some experimental evidence for shape coexistence in  $^{190}\text{W}_{114}$  [5,6]. The transitional region in the case of the platinum ( $Z = 78$ ) nuclei starts at around mass  $A = 192$  and persists till  $A \approx 200$  [7]. These nuclei are understood to have axially asymmetric shapes and they are considered to

present the best examples of  $\gamma$ -softness throughout the whole nuclide chart [8]. In the case of osmium nuclei ( $Z = 76$ ) the prolate-oblate shape change is predicted to be a sudden one [7,9]. The exact place where this change occurs for the ground state of the osmium isotopes is not clear. Experimental information suggests that up to mass  $A = 194$  the osmium isotopes are prolate [10], but the  $\gamma$  degree of freedom is also important [11]. In  $^{196}\text{Os}_{116}$  the available experimental information is too scarce to draw a definite conclusion, as only two excited states were observed [7].

Despite the intense theoretical interest in the shape transitional W-Pt region, this is the part of the nuclide chart with the least information on neutron-rich nuclei. The high sensitivity achievable in the isomeric decay experiments and the recent increase in relativistic energy primary beam intensities have opened up new possibilities. Here we present the first experimental information on  $^{198}_{76}\text{Os}_{122}$ .

Heavy nuclear species were populated in relativistic energy projectile fragmentation. A beryllium target of thickness  $2.5 \text{ g/cm}^2$  was bombarded with an  $E/A = 1 \text{ GeV}$ ,  $^{208}\text{Pb}$  beam provided by the SIS accelerator at GSI, Darmstadt, Germany. The typical, on-target beam intensity was  $(0.5\text{--}1.0) \times 10^9$  lead

\*Corresponding author: [Z.Podolyak@surrey.ac.uk](mailto:Z.Podolyak@surrey.ac.uk)

ions per  $\approx 8$ -s long spill. The spills were separated by  $\approx 18$ -s periods without beam. The nuclei of interest were separated and identified by using the FRagment Separator (FRS) [12] operated in standard achromatic mode with a wedge-shaped aluminium degrader in the intermediate focal plane. The transmitted ions were slowed in a variable thickness aluminium degrader and finally stopped in a 9-mm-thick plastic (perspex) catcher. The catcher was surrounded by the high-efficiency, high-granularity stopped RISING  $\gamma$ -ray spectrometer [13], which has a full-energy peak efficiency of 15% at 662 keV. Time-correlated  $\gamma$  decays from individually identified ions have been measured, allowing unambiguous identification of isomeric decays. For details of the identification procedure and the setup used in the present experiment see Refs. [4,14].

The results for  $^{198}\text{Os}$  were obtained from two different magnetic rigidity settings. Approximately half of the data comes from a setting optimized to select fully stripped ions centered on the maximal transmission of  $^{199}\text{Os}$ ; the other half comes from a setting centered on  $^{203}\text{Ir}$ .

A total of  $7.8 \times 10^4$   $^{198}\text{Os}$  ions were implanted in the catcher. The detection of the previously identified  $\gamma$  rays following the de-excitation of isomeric states in  $^{200}\text{Pt}$  [15],  $^{201,202}\text{Pt}$ ,  $^{193}\text{Re}$ ,  $^{195}\text{Os}$ , and  $^{198}\text{Ir}$  [16] were used to confirm the calibration of the particle identification.

The total  $\gamma$ -ray spectrum observed in delayed coincidence with  $^{198}\text{Os}$  ions is shown in Fig. 1. The high efficiency of the RISING array and the large number of identified  $^{198}\text{Os}$  nuclei allowed the determination of the coincidence relationships between the observed  $\gamma$  rays (see the bottom part of Fig. 1). Based on the  $\gamma$ -ray intensities and the coincidence relations the level scheme shown in Fig. 2 has been built. All the  $\gamma$  rays placed in the level scheme of Fig. 2 show a similar time behavior, suggesting that they are fed from the depopulation of the same isomeric state. The extracted half-life of the isomer is  $T_{1/2} = 16(1)$  ns (see inset of Fig. 1). This lifetime is much shorter than the flight time between the production target and

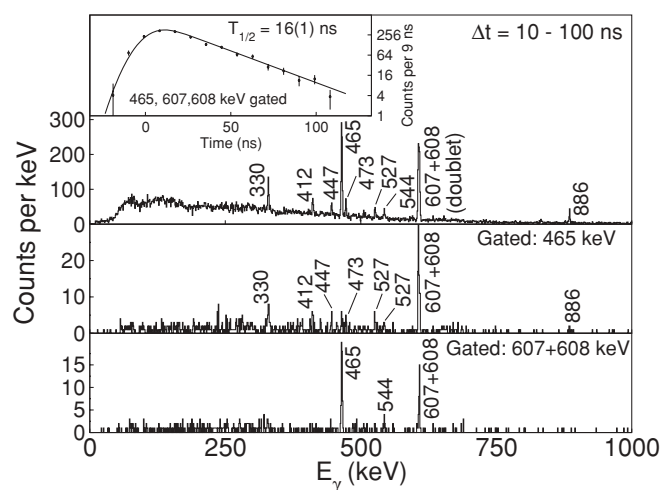


FIG. 1. Delayed  $\gamma$ -ray spectra associated with  $^{198}\text{Os}$ . (Top) Singles spectrum taken within 100 ns after implantation. The inset shows the time spectrum associated with the strongest  $\gamma$ -ray transitions. (Bottom) Coincidence spectra obtained by gating on the 465-keV and (607 + 608)-keV transitions.

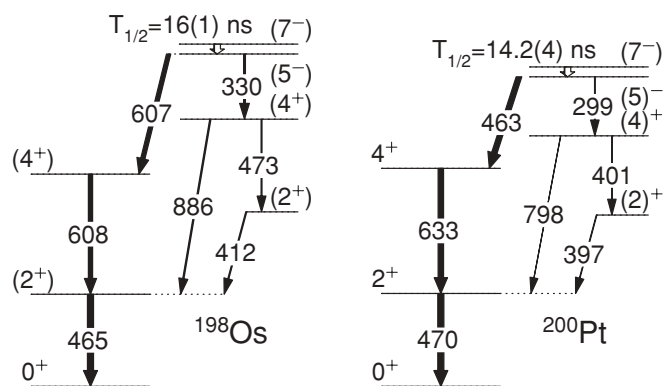


FIG. 2. Proposed level scheme of  $^{198}\text{Os}$ . For comparison the partial level scheme of the  $N = 122$  isotone  $^{200}\text{Pt}$  is also shown [15–17]. The unobserved  $(7^-) \rightarrow (5^-)$  transitions are estimated to have energies of  $< 90$  keV.

the detection position ( $\approx 230$  ns). The survival of the nucleus in its isomeric state indicates that the decay-out transition has a large electron conversion coefficient and is therefore of low energy. This unobserved transition is estimated to have an energy of less than 90 keV. The spin-parity values of the excited states are tentative and are based on both systematics and theoretical considerations. For comparison, the partial level scheme of the  $N = 122$  isotone  $^{200}\text{Pt}$  [15–17] is also shown in Fig. 2. The low-intensity 447-, 527-, and 544-keV transitions shown in Fig. 1 are in tentative coincidence relationships with each other and all the other  $\gamma$  rays placed in the level scheme of Fig. 2. They must originate from a higher lying isomer, with an extracted half-life of  $T_{1/2} = 18(3)$  ns.

We note that during the present experiment the  $^{196}\text{Os}$  nucleus was also produced and implanted in the catcher. Despite of the large statistics ( $121 \times 10^3$  implanted  $^{196}\text{Os}$  nuclei compared to  $78 \times 10^3$  of  $^{198}\text{Os}$ ), no evidence of isomeric decay was found. This suggests that in  $^{196}\text{Os}$  the  $7^-$  state lies at least 100 keV higher in energy than the  $5^-$  state, and it decays during the flight time within the fragment separator. The other possible scenario, that the  $7^-$  is below the  $5^-$ , would result in a  $7^-$  isomer with a half-life of hundreds of microseconds (as is in the case of  $^{202}\text{Pt}$  [16]) and it should be observable with the present setup.

Isomeric states with  $I^\pi = 7^-$  have been reported in the even  $A = 196$ – $202$  platinum isotopes [15,16,18,19]. They were interpreted as having a mixed two-proton  $\pi h_{11/2}d_{3/2}$  and two-neutron  $\nu i_{13/2}p_{1/2}$  character. Whereas in  $^{196}\text{Pt}$  the two-neutron component is stronger [18], in the heavier platinum nuclei the two protons are dominant [16,19]. In  $^{196,198,200}\text{Pt}$  the  $7^-$  isomers decay into the yrast  $\pi h_{11/2}s_{1/2}5^-$  state by a low-energy transition with  $E2$  character. The half-lives are in the range of nanoseconds, and the  $B(E2; 7^- \rightarrow 5^-)$  transition strengths in the region of 15–25 W.u., decreasing with mass. Based on the similarities between the level structure of the  $^{196}$ – $^{200}\text{Pt}$  isotopes and the  $^{198}\text{Os}$  nucleus we suggest that in  $^{198}\text{Os}$  the isomeric state has  $\pi h_{11/2}d_{3/2}$  character and  $I^\pi = 7^-$ , and it decays via a low-energy transition into the  $5^-$  state with  $\pi h_{11/2}s_{1/2}$  configuration. The determined transition strength is  $B(E2; 7^- \rightarrow 5^-) = 15(5)$  W.u. We note that there is a lack

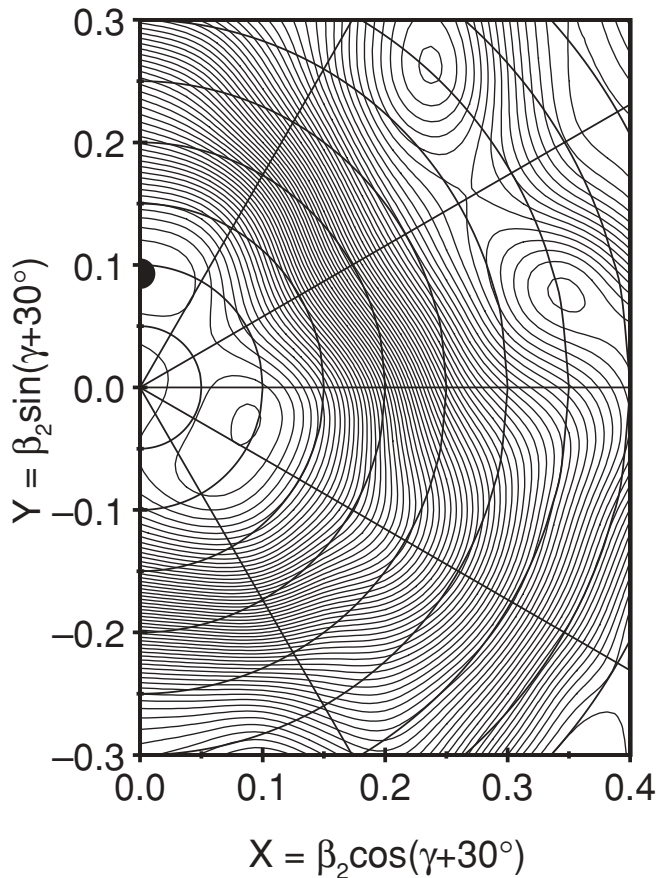


FIG. 3. Potential energy surface calculations for the ground state of  $^{198}\text{Os}$ . The energy difference between two successive contour lines is 200 keV. The calculations indicate a shape with deformation parameters  $\beta_2 = 0.093$ ,  $\beta_4 = -0.028$ , and  $\gamma = 60^\circ$  (black dot).

of sensitivity of the transition strength to the transition energy owing to the large effect of the electron conversion. The higher lying isomer in  $^{198}\text{Os}$  observed here is very similar in its decay pattern and half-life to that observed in  $^{200}\text{Pt}$  [16] and it probably has fully aligned  $\nu i_{13/2}^2$  character with  $I^\pi = 12^+$ . Excited states with this structure were identified in less neutron rich platinum and mercury isotopes [20,21] as well.

The oblate-prolate shape transition in the Hf-Pt region has been theoretically studied with several approaches. Mean-field calculations have been performed with different interactions. For example, self-consistent axially deformed Hartree-Fock calculations with a separable monopole interaction predict prolate shape for osmium isotopes with  $A \leq 190$  and oblate shape for  $^{192-198}\text{Os}$  [2]. However, mean-field calculations performed by Sarriguren *et al.* [1], Ansari [9], and Naik *et al.* [22] using a range of approximations predict that the lightest oblate isotope is  $^{194}\text{Os}$ ,  $^{196}\text{Os}$ , or  $^{198}\text{Os}$ , depending on the approach employed.

The interacting boson model (IBM) is often employed to describe the properties of transitional nuclei. It is considered that the platinum nuclei are close to the  $O(6)$  limit, which corresponds to a  $\gamma$  unstable shape, with  $^{196}\text{Pt}$  being the best example of this symmetry [23]. Recently, Jolie and Linnemann [24] successfully described a range of nuclear properties in

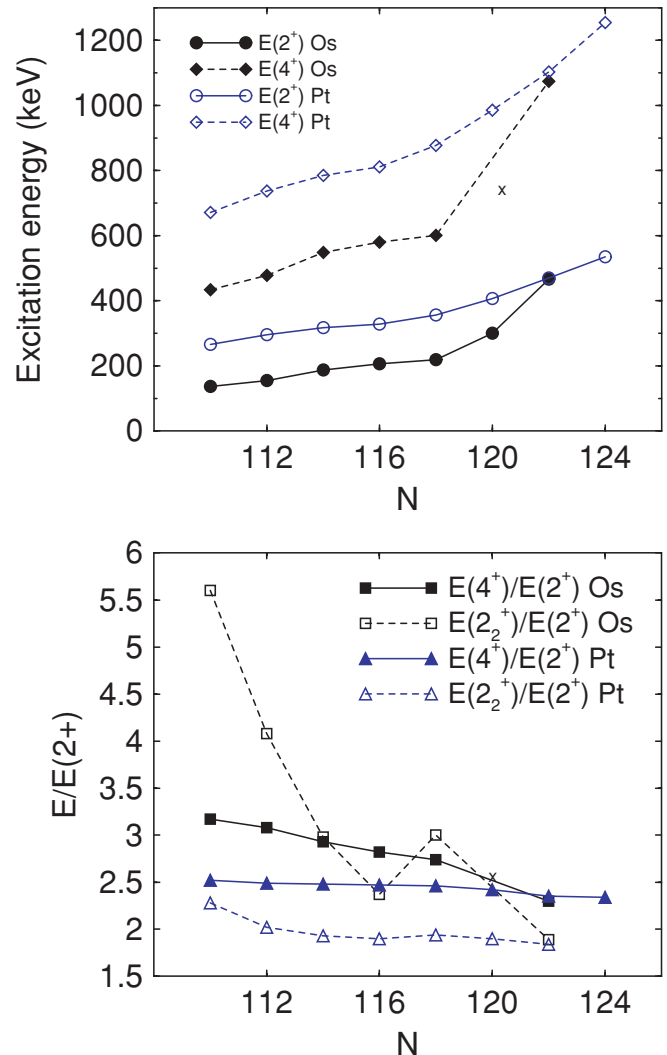


FIG. 4. (Color online) Systematics of the  $E(2^+)$  and  $E(4^+)$  energies and the  $E(4^+)/E(2^+)$  and  $E(2_2^+)/E(2^+)$  energy ratios in the even mass  $A = 188-202$  osmium and platinum isotopes. The values corresponding to the second excited state in  $^{196}\text{Os}$ , which is either the yrast  $4^+$  or the second  $2^+$  state, are indicated with the symbol x.

the Hf-Hg region, including the quadrupole moments that are directly related to the shape. It was shown that there is a prolate-oblate  $SU(3)-\overline{SU(3)}$  phase transition predicted in this region.

Here, Woods-Saxon-Strutinsky calculations have been performed, as described in Ref. [25]. This type of calculation has been extensively employed and has proved successful in this mass region [5,10]. The potential energy minimization has been done in the three-dimensional deformation space of  $\beta_2$ ,  $\beta_4$ , and  $\gamma$ . Axially symmetric prolate shapes correspond to  $\gamma = 0^\circ$ , whereas noncollective oblate shapes correspond to  $\gamma = 60^\circ$ . For  $^{198}\text{Os}$  the calculations indicate a very soft system in both  $\gamma$  and  $\beta$  degrees of freedom, with a minimum corresponding to weak oblate deformation with parameters  $\beta_2 = 0.093$ ,  $\beta_4 = -0.028$ , and  $\gamma = 60^\circ$  (see Fig. 3). The same type of calculation performed for lighter osmium isotopes indicates a prolate shape for  $^{190,192,194}\text{Os}$ , with decreasing

quadrupole deformation for increasing mass, and an oblate shape with  $\beta_2 = 0.12$  for  $^{196}\text{Os}$  [10].

The yrast structures of  $^{190,192,194}\text{Os}$  nuclei were observed up to at least spin-parity  $10^+$ . They are well understood by considering a prolate shape. The prolate character of  $^{194}\text{Os}$  is consistent with the nonobservation of back-bending before  $10^+$  [10].  $^{196}\text{Os}$  is the heaviest osmium isotope where excited states were previously observed [7]. It was populated in the  $^{198}\text{Pt}(^{14}\text{C}, ^{16}\text{O})$  reaction and excited states with energies of 300(20) and 760(20) keV were observed. Although the first excited state is almost certainly the yrast  $2^+$ , the other observed state could be either the second  $2^+$  or the yrast  $4^+$  state. It was inferred from the high  $E(2^+)$  energy that this nucleus is significantly less deformed than the lighter prolate isotopes.

The energies of the lowest excited states can be used to infer information about the character of the nuclei. Systematics related to the yrast  $2^+$  and  $4^+$  states as well the second  $2^+$  state ( $2_2^+$ ) are presented in Fig. 4. In  $^{198}\text{Os}$ , the ordering of the coincident 412- and 473-keV transitions cannot be determined from the present experiment. Here we considered the ordering shown in Fig. 2, resulting in an  $E(2_2^+)/E(2^+)$  energy ratio of 1.89. By changing the order of the transitions the ratio is slightly modified to 2.02. This assumption does not have any consequences on the discussion that follows. As shown in Fig. 4, the platinum energies change slowly with atomic mass. The yrast  $E(2^+)$  and  $E(4^+)$  energies increase smoothly, and the  $E(4^+)/E(2^+)$  energy ratio remains constant at about 2.5, the ratio expected for perfect O(6)  $\gamma$ -soft nuclei. The  $E(2_2^+)/E(2^+)$  energy ratio is smoothly decreasing and has a value of around  $\sim 2$ . In contrast to the platinum nuclei, in the osmium isotopes there is a sudden change at around  $A = 196$ . The large  $E(4^+)/E(2^+)$  energy ratio and the smooth change of the yrast  $E(2^+)$  and  $E(4^+)$  energies in the case of the

$A = 188\text{--}194$  osmium nuclei indicate that these isotopes are deformed. At  $A = 196$  there is an abrupt increase in the energy of the  $2^+$  state. This is even more obvious in the case of  $^{198}\text{Os}$ , where both the  $E(4^+)$  and  $E(2^+)$  energies are much higher than in the lighter Os nuclei. Similarly, the  $E(4^+)/E(2^+)$  and  $E(2_2^+)/E(2^+)$  energy ratios drop to the lowest values for the osmium isotopes in the region. The low  $E(4)/E(2)$  ratio is consistent with a low deformation and is less than the predicted 2.5 for  $\gamma$ -soft O(6) nuclei, whereas the low  $E(2_2^+)/E(2^+)$  ratio also indicates the  $\gamma$ -softness of the system.

In conclusion, excited states in the neutron-rich  $^{198}\text{Os}$  nucleus have been identified following internal decays of isomeric states populated in relativistic energy fragmentation reactions. The energies of the yrast  $2^+$  and  $4^+$  states suggest a weakly deformed character, and the low energy of the second  $2^+$  state is consistent with the  $\gamma$ -softness characteristic to this mass region. This interpretation is compatible with the theoretical calculations predicting  $^{198}\text{Os}$  to be a weakly deformed oblate nucleus. The sudden drop in  $E(2_2^+)/E(2^+)$  for  $A > 194$  osmium isotopes might be a signature of a prolate-to-oblate shape change, but more detailed theoretical calculations are needed to clarify this surprising feature.

The excellent work of the GSI accelerator staff is acknowledged. This work is supported by the STFC/EPSRC (UK) and AWE plc. (UK), the EU Access to Large Scale Facilities Programme (EURONS, EU Contract No. 506065), the Swedish Research Council, the Polish Ministry of Science and Higher Education (Grant Nos. 1 P03B 030 30 and N N202 309135), the Bulgarian Science Fund, the US DOE (Grant No. DE-FG02-91ER-40609), the Spanish Ministerio de Educacion y Ciencia, the German BMBF, the Hungarian Science Foundation, and the Italian INFN.

- 
- [1] P. Sarriguren, R. Rodriguez-Guzmán, and L. M. Robledo, *Phys. Rev. C* **77**, 064322 (2008).
- [2] P. D. Stevenson, M. P. Brine, Zs. Podolyák, P. H. Regan, P. M. Walker, and J. R. Stone, *Phys. Rev. C* **72**, 047303 (2005).
- [3] K. H. Maier *et al.*, *Phys. Rev. C* **30**, 1702 (1984).
- [4] S. Steer *et al.*, *Phys. Rev. C* **78**, 061302 (2008).
- [5] Zs. Podolyák *et al.*, *Phys. Lett.* **B491**, 225 (2000).
- [6] P. M. Walker and F. R. Xu, *Phys. Lett.* **B635**, 285 (2006).
- [7] P. D. Bond, R. F. Casten, D. D. Warner, and D. Horn, *Phys. Lett.* **B130**, 167 (1983).
- [8] R. F. Casten, *Nuclear Structure from a Simple Perspective* (Oxford University Press, New York, 1990); 2nd Ed. (Oxford University Press, 2000), p. 463.
- [9] A. Ansari, *Phys. Rev. C* **33**, 321 (1986).
- [10] C. Wheldon *et al.*, *Phys. Rev. C* **63**, 011304(R) (2000).
- [11] C. Y. Wu and D. Cline, *Nucl. Phys.* **A607**, 178 (1996).
- [12] H. Geissel *et al.*, *Nucl. Instrum. Methods Phys. Res. B* **70**, 286 (1992).
- [13] S. Pietri *et al.*, *Nucl. Instrum. Methods B* **261**, 1079 (2007); P. H. Regan *et al.*, *Nucl. Phys.* **A787**, 491c (2007).
- [14] Zs. Podolyák *et al.*, *Eur. Phys. J. Spec. Top.* **150**, 165 (2007).
- [15] S. Yates *et al.*, *Phys. Rev. C* **37**, 1889 (1988).
- [16] M. Caamano *et al.*, *Eur. Phys. J. A* **23**, 201 (2005).
- [17] F. G. Kondev and S. Lalkovski, *Nucl. Data Sheets* **108**, 1471 (2007).
- [18] X. Huang, *Nucl. Data Sheets* **108**, 1093 (2007).
- [19] C. Zhou, *Nucl. Data Sheets* **95**, 59 (2002); P. Schuler *et al.*, *Z. Phys. A* **317**, 313 (1984).
- [20] J. J. Valiente-Dobón *et al.*, *Phys. Rev. C* **69**, 024316 (2004).
- [21] C. Günther *et al.*, *Phys. Rev. C* **15**, 1298 (1977).
- [22] Z. Naik *et al.*, *Pramana J. Phys.* **62**, 827 (2004).
- [23] J. A. Cizewski *et al.*, *Phys. Rev. Lett.* **40**, 167 (1978).
- [24] J. Jolie and A. Linnemann, *Phys. Rev. C* **68**, 031301(R) (2003).
- [25] W. Nazarewicz *et al.*, *Nucl. Phys.* **A435**, 397 (1985).